Oxygen Transport Ceramic Membranes

Quarterly Report

July 2004 – Sept 2004

Principal Authors:

Prof. S. Bandopadhyay

Dr. N. Nagabhushana

Issued: October 2004

DOE Award # DE-FC26-99FT40054

University of Alaska Fairbanks
Fairbanks, AK 99775

Contributing sub contractors:

1. **X.-D Zhou, Q. Cai, J. Yang, W. B. Yelon, W. J. James and H. U. Anderson,** Materials Research Center, University of Missouri-Rolla, Rolla, MO 65401
2. **Prof. Alan Jacobson and Prof. C.A. Mims;** University of Houston/University of Toronto

DISCLAIMER

ABSTRACT

The present quarterly report describes some of the investigations on the structural properties of dense OTM bars provided by Praxair and studies on newer composition of Ti doped LSF.

In this report, Mössbauer spectroscopy was used to study the local environmentals of LSFT with various level of oxygen deficiency. Ionic valence state, magnetic interaction and influence of Ti on superexchange are discussed

Stable crack growth studies on Dense OTM bars provided by Praxair were done at elevated temperature, pressure and elevated conditions. Post-fracture X-ray data of the OTM fractured at 1000ºC in environment were refined by FullProf code and results indicate a distortion of the parent cubic perovskite to orthorhombic structure with reduced symmetry. TGA-DTA studies on the post-fracture samples also indicated residual effect arising from the thermal and stress history of the samples.

An electrochemical cell has been designed and built for measurements of the Seebeck coefficient as a function of temperature and pressure. The initial measurements on $La_{0.2}Sr_{0.8}Fe_{0.55}Ti_{0.45}O_{3-\delta}$ are reported. Neutron diffraction measurements of the same composition are in agreement with both the stoichiometry and the kinetic behavior observed in coulometric titration measurements. A series of isotope transients under air separation mode (small gradient) were completed on the membrane of LSCrF-2828 at 900°C. Low pO_2 atmospheres based on with CO - CO_2 mixtures have also been admitted to the delivery side of the LSCrF-2828 membrane to produce the gradients which exist under syngas generation conditions. The CO - CO_2 mixtures have normal isotopic ^{18}O abundances. The evolution of ^{18}O on the delivery side in these experiments after an ^{18}O pulse on the air side reveals a wealth of information about the oxygen transport processes.

TABLE OF CONTENTS

LIST OF GRAPHICAL MATERIALS

INTRODUCTION

Conversion of natural gas to liquid fuels and chemicals is a major goal for the Nation as it enters the 21st Century. Technically robust and economically viable processes are needed to capture the value of the vast reserves of natural gas on Alaska's North Slope, and wean the Nation from dependence on foreign petroleum sources. Technologies that are emerging to fulfill this need are all based syngas as an intermediate. Syngas (a mixture of hydrogen and carbon monoxide) is a fundamental building block from which chemicals and fuels can be derived. Lower cost syngas translates directly into more cost-competitive fuels and chemicals.

The currently practiced commercial technology for making syngas is either steam methane reforming (SMR) or a two-step process involving cryogenic oxygen separation followed by natural gas partial oxidation (POX). These high-energy, capital-intensive processes do not always produce syngas at a cost that makes its derivatives competitive with current petroleum-based fuels and chemicals.

In the mid 80's BP invented a radically new technology concept that will have a major economic and energy efficiency impact on the conversion of natural gas to liquid fuels, hydrogen, and chemicals.[1] This technology, called Electropox, integrates oxygen separation with the oxidation and steam reforming of natural gas into a single process to produce syngas with an economic advantage of 30 to 50 percent over conventional technologies.[2]

The Electropox process uses novel and proprietary solid metal oxide ceramic oxygen transport membranes [OTMs], which selectively conduct both oxide ions and electrons through their lattice structure at elevated temperatures.[3] Under the influence of an oxygen partial pressure gradient, oxygen ions move through the dense, nonporous membrane lattice at high rates with

---

[1]Mazanec, T. J.; Cable, T. L.; Frye, J. G., Jr.; US 4,793,904, 27 Dec **1988**, assigned to The Standard Oil Company (now BP America), Mazanec, T. J.; Cable, T. L.; US 4,802,958, 7 Feb **1989**, assigned to the Standard Oil Co. (now BP America), Cable, T. L.; Mazanec, T. J.; Frye, J. G., Jr.; European Patent Application 0399833, 24 May **1990**, published 28 November **1990.**

[2]Bredesen, R.; Sogge, J.; "A Technical and Economic Assessment of Membrane Reactors for Hydrogen and Syngas Production" presented at Seminar on the Ecol. Applic. of Innovative Membrane Technology in the Chemical Industry", Cetraro, Calabria, Italy, 1-4 May **1996**.

[3]Mazanec, T.J., *Interface*, **1996**; Mazanec, T.J., *Solid State Ionics*, 70/71, **1994** 11-19; "Electropox: BP's Novel Oxidation Technology", T.J. Mazanec, pp 212-225, in "The Role of Oxygen in Improving Chemical Processes", M. Fetizon and W.J. Thomas, eds, Royal Society of Chemistry, London, **1993**; "Electropox: BP's Novel Oxidation Technology", T.J. Mazanec, pp 85-96, in "The Activation of Dioxygen and Homogeneous Catalytic Oxidation", D.H.R. Barton, A. E. Martell, D.T. Sawyer, eds, Plenum Press, New York, **1993**; "Electrocatalytic Cells for Chemical Reaction", T.J. Mazanec, T.L. Cable, J.G. Frye, Jr.; Prep Petrol Div ACS, San Fran, **1992** *37*, 135-146; T.J. Mazanec, T.L. Cable, J.G. Frye, Jr.; *Solid State Ionics*, **1992**, 53-56, 111-118.

100 percent selectivity. Transported oxygen reacts with natural gas on the fuel side of the ceramic membrane in the presence of a catalyst to produce syngas.

In 1997 BP entered into an OTM Alliance with Praxair, Amoco, Statoil and Sasol to advance the Electropox technology in an industrially sponsored development program. These five companies have been joined by Phillips Petroleum and now are carrying out a multi-year $40+ million program to develop and commercialize the technology. The program targets materials, manufacturing and engineering development issues and culminates in the operation of semi-works and demonstration scale prototype units.

The Electropox process represents a truly revolutionary technology for conversion of natural gas to synthesis gas not only because it combines the three separate unit operations of oxygen separation, methane oxidation and methane steam reforming into a single step, but also because it employs a chemically active ceramic material in a fundamentally new way. On numerous fronts the commercialization of Electropox demands solutions to problems that have never before been accomplished. Basic problems in materials and catalysts, membrane fabrication, model development, and reactor engineering all need solutions to achieve commercial success.

Six important issues have been selected as needing understanding on a fundamental level at which the applied Alliance program cannot achieve the breadth and depth of understanding needed for rapid advancement. These issues include:

1. Oxygen diffusion kinetics (University of Houston);
2. Phase stability and stress development (University of Missouri - Rolla);
3. Mechanical property evaluation in thermal and chemical stress fields (University of Alaska Fairbanks)

Statement of Work

Task 1 *Evaluate phase stability and thermal expansion of candidate perovskite membranes and develop techniques to support these materials on porous metal structures.*

Task 2 *Determine materials mechanical properties under conditions of high temperatures and reactive atmospheres.*

Task 3 *Measure kinetics of oxygen uptake and transport in ceramic membrane materials under commercially relevant conditions using isotope labeling techniques.*

EXECUTIVE SUMMARY

Research on the Oxygen Transport Membranes as listed as tasks 1-3 are being performed at the various universities under the stewardship of Praxair. The quarterly technical report presents the progress of the tasks defined to understand the fundamental concepts and structural performance of the OTM material.

It is of interest to that unlike the LSF series, the changes of lattice parameters for LSFT in air and nitrogen are not obvious. Unit cell volume as a function of lattice parameter also indicates the similar behavior. The obvious answer seems to be the substitution of Ti into LSF. This still did not resolve the reason for Ti to stabilize the structure upon changing gas environments. Further work will be aimed at understanding this phenomenon by using thermogravimetric analysis and transport measurements.

Stable crack growth studies on Dense OTM bars provided by Praxair were done at elevated temperature/pressure and N_2 environment. Post fracture evaluation indicated stable crack growth from the indent and microscopic observation clearly indicated an indented region, a regime of slow and stable crack growth, fast fracture and compression curl in the tested sample. New TGA-DTA studies on the post-fracture samples with an annealing cycle to remove the residual effect arising from the thermal and stress history of the sample indicated behavior similar to many of these classes of materials. The results indicate that there is a further change in stoichiometry of the OTM membrane fractured at elevated pressures as compared to related studies on non pressurized fractured samples.

We have continued to investigate the thermodynamic properties (stability and phase-separation behaviour) and total conductivity of prototype membrane materials. The data are needed together with the kinetic information to develop a complete model for the membrane transport. We have previously reported characterization, stoichiometry, conductivity, and dilatometry measurements for samples of $La_{0.2}Sr_{0.8}Fe_{0.55}Ti_{0.45}O_{3-x}$. In this period, we have designed and constructed an electrochemical cell for measurement of the Seebeck coefficient and report some initial results. In situ neutron diffraction measurements on $La_{0.2}Sr_{0.8}Fe_{0.55}Ti_{0.45}O_{3-\delta}$ were made at Argonne National Laboratory in collaboration with Yaping Li, J. Jorgensen, and J. Richardson. Measurements were made at three temperatures and at different oxygen partial pressures. The response of the lattice parameter to changes in oxygen partial pressure was determined. At high pO_2 values the response of the sample to changing the pO_2 is fast whereas below 10^{-4} atm the response is very slow. The response rate increase again when the pressure is dropped to 10^{-14} atm. These results mirror the previous stoichiometry and conductivity observations on this material and on other ferrites that all show very slow kinetics in the

intermediate pressure range. The data suggest some non-equilibrium behavior which is most likely associated with cation diffusion or rearrangement of microdomains.

In the area of isotope transient studies at steady state, the current quarter has been dominated by analysis of the data from the isotope transients and the analysis of the profile in the quenched membrane. Air separation transients were fit to the 1-D transport model. The oxygen diffusivity did not show a significant dependence on the average oxygen activity in the membrane over the modest range used. The derived values of the forward oxygen surface activation rate coefficient for the same transients were obtained as function of the air-side oxygen partial pressure. Some variability with the value of the oxygen partial pressure on the delivery side was observed but the expected systematic variation, showing higher forward rate coefficients with increasing gradient across the membrane was not evident in the data. The first high gradient experiment involved a sweep gas with $Ar:CO_2:CO = 90:10:1$. Molecular oxygen appeared on the sweep side of the membrane. Oxygen recombination was sufficiently fast to compete with CO oxidation for oxygen removal on the sweep side. The activity gradient in the membrane was therefore modest and similar to the air separation experiments. When the gas admitted was 50% CO, the membrane switched to high gradient – high flux mode. The time scale is much shorter, in agreement with the substantially higher oxygen flux and no molecular oxygen is seen. If the entire delivery surface is at sufficient low oxygen potential, molecular oxygen formation is thermodynamically prohibited, consistent with our observations. At the end of the experiment the membrane was quenched and cut for profile measurements. Oxygen – 18 SIMS maps of the cross section of the membrane have been obtained and are currently being modeled.

Task 1: Preparation and Characterization of Dense Ceramic oxygen Permeable Membranes

X.-D Zhou[1], Q. Cai[2], J. Yang[1], W. B. Yelon[1], W. J. James[1] and H. U. Anderson[1]

1. **Materials Research Center, University of Missouri-Rolla, Rolla, MO 65401**
2. **Department of Physics, University of Missouri-Columbia, Columbia, MO 65211**

In situ Neutron Diffraction Analysis of $La_{0.2}Sr_{0.8}Fe_{0.55}Ti_{0.45}O_{3-\delta}$ - N_2

Experimental

L2SF55T specimen was sintered at 1400ºC for 2 hours and then cooling to room temperature at 3ºC/min. The bar samples were then annealed at temperatures from 800 – 1500ºC for 24hours, followed by a quench to room temperature. The quenched samples have been used for neutron diffraction measurements. Mössbauer spectra were measured using a source of ^{57}Co in a Rh matrix with a conventional constant accelerated driver. A standard α - Fe was used to calibrate the spectrometer with the isomer shift relative to α - Fe at 300K.

Results and Discussion

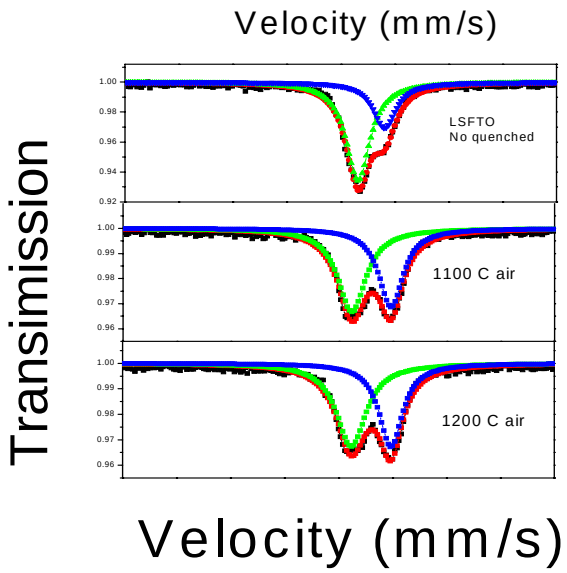

Fig. 1. (a) Mössbauer spectra of LSFT samples quenched from 1100ºC and 1200ºC to room temperature. A spectrum of LSFT is included, which was annealed at 1400ºC and cooled to room temperature at 3ºC/min.

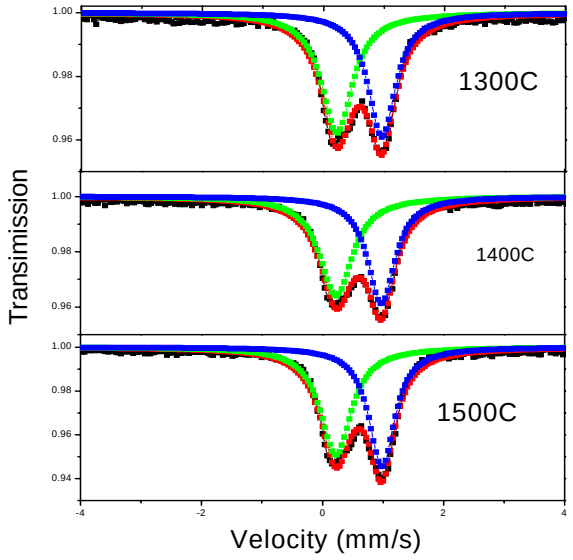

Fig. 1 (b) Mössbauer spectra of LSFT samples quenched from 1300ºC, 1400ºC and 1500ºC to room temperature.

Fig. 1 (a) and (b) show the Mössbauer spectra of LSFT specimens quenched to room temperature from annealing temperatures ranging from 1100 to 1500ºC. Included in Fig. 1(a) is a spectrum of the sample cooled from 1400ºC at 3ºC/min to room temperature. All of the spectra possess two singlet peaks, which indicate the paramagnetic interaction at room temperature for these materials. We know that the isomer shift arises from the interaction energy of the part of the electronic cloud, inside the nucleus, with the nuclear charge. Thus, Mössbauer spectra can provide direct information on the electron density at the nucleus and this can often be interpreted to give unequivocal information about the valence state of the Fe ion. Hence, these two sets of singlet spectra in Fig. 1 show that there exist two distinguish local environments for Fe ions in LSFT, which is often interpreted as valence state. From previous reported results, we anticipated these two valence states are in 3+ and 4+. Fig. 2 illustrates a detailed analysis of isomer shift as a function of quenching temperature for LSFT. Fig. 3 shows a plot of fraction of two Fe ions in quenched LSFT. The oxygen vacancy density increases with increasing quenching temperature, which reduces the fraction of Fe 4+ ions. This implies that Fe

ions responsible for isomer shift labeled Fe(1) in Fig. 3 should correspond to Fe 4+ and Fe(2) represents Fe 3+ in Fig. 3.

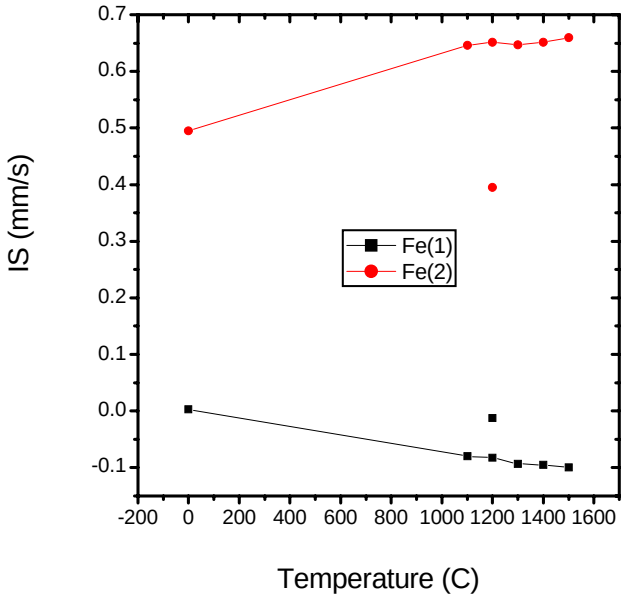

Fig. 2. Isomer shift of two types of Fe ions in LSFT quenched to room temperature from the temperatures ranging between 1100 and 1500ºC. Included is the isomer shift of the specimen, which was annealed at 1400ºC and then cooled to room temperature at 3ºC/min.

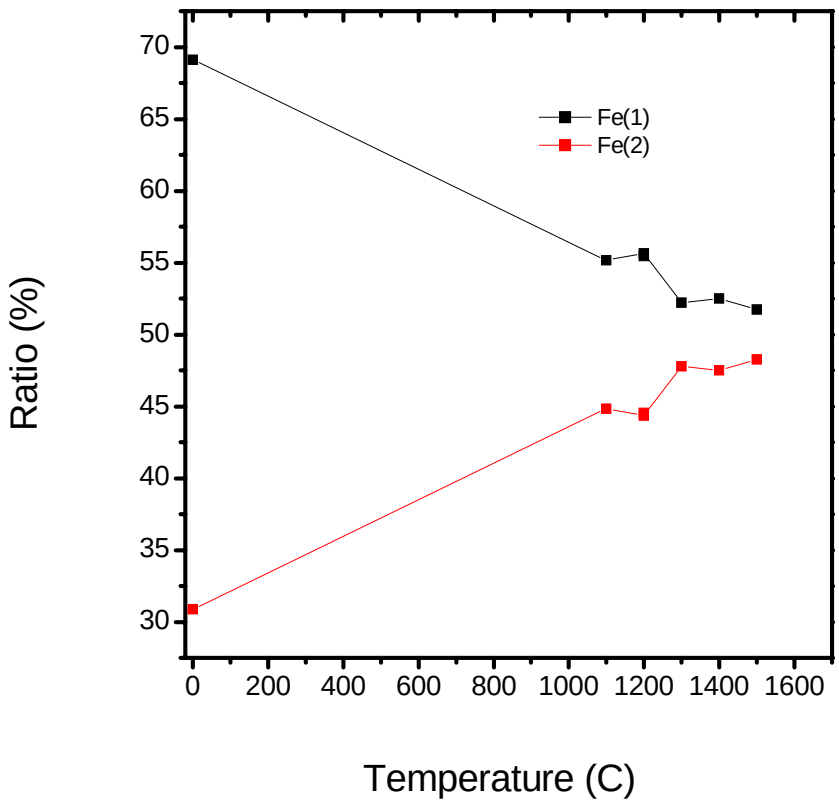

Fig. 3. The fraction of two types of Fe ions in LSFT quenched to room temperature from the temperatures ranging between 1100 and 1500ºC. Included is the Fe ion fraction in the specimen which was annealed at 1400ºC and then cooled to room temperature at 3ºC/min.

TASK 2: Determine material mechanical properties under conditions of high temperature and reactive atmosphere

Prof. Sukumar Bandopadhyay and Dr. Nagendra Nagabhushana

University of Alaska Fairbanks

In this quarter, studies were continued on dense OTM bar samples received from Praxair. A new fixture was designed to provide sharp pre-crack and stable crack growth studies were performed. X-ray data was refined for deriving lattice parameters and TG-DTA analysis were performed on post-fracture specimens.

Experimental:

In the previous quarter, results from the TGA/DTA studies were assumed to be artifacts of prior thermal/stress history in the specimen. Based on discussions with the group at University of Houston, a thermal profile was added in the test run to negate the so-called history effects.

For this the specimens, were rapidly heated in N_2 up to 1000°C and cooled to 100°C. For comparative purpose, test runs similar to earlier studies were done.

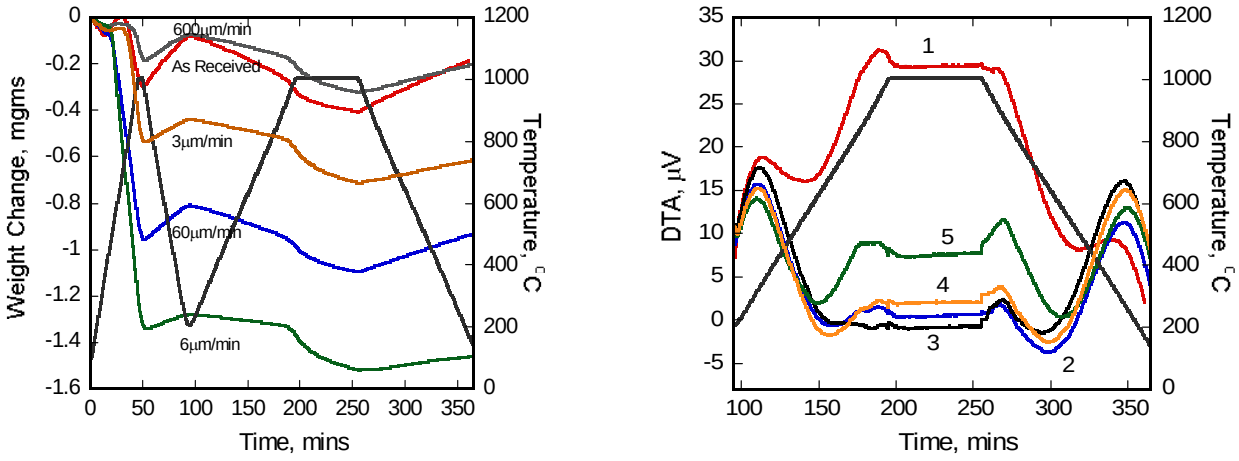

Fig 4: TGA/DTA run on samples with prior thermal/stress history negated by initial heating in N_2.
1: As received, 2: 600µm/min, 3:60µm/min, 4: 6µm/min and 5: 3µm/min

Results from the new test runs, confirmed the expected presence of residual effects in the sample due to prior thermal/stress history. As shown in Fig. 4a and b, the first heat up cycle indicated significant weight loss as reported in earlier studies and the second cycle showed the expected

behavior from these classes of materials. However, the TGA/DTA signal still reflected on possible changes in the material which may not be reversible.

Crack Growth studies under elevated temperature and pressure:

First studies were done on evaluating crack growth in OTM membranes under combined temperature, pressure and environment loading. Precrack in the flexure bar were initiated by the indentation-bridge technique as described in the earlier report.

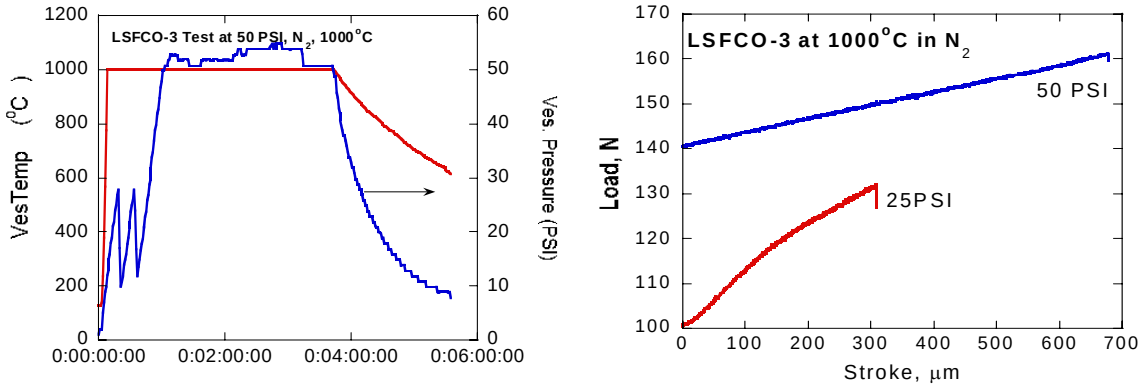

Fig 5: a) Combined Temperature/Pressure test run to evaluate crack growth in OTM membranes. b) Increase in hydrostatic pressure leads to increased stress for crack growth and final fracture.

Fig 6: Fracture in OTM membranes under combined elevated temperature and pressure loading. The fracture origins are at the multiple indents placed on the tensile surface.

As shown in Fig 5 and 6, the methodology used for crack growth and fracture studies at room temperature are fairly reproduced at elevated temperature and pressure conditions. This is an important aspect as the safety and alignment procedures are very critical for studies under such conditions. This is also the first available data points on these classes of materials in more practical conditions.

Under the conditions mentioned above, the fracture stress of the OTM membrane materials appear to increase under elevated hydrostatic pressure. Previous studies have indicated that, the surface cracks may blunt or often close upon exposure to reducing environment (N_2 ~10^{-4} and above). This effect may be further magnified in the presence of hydrostatic pressure resulting in increased strength and changes in crack growth behavior.

X-Ray analysis:

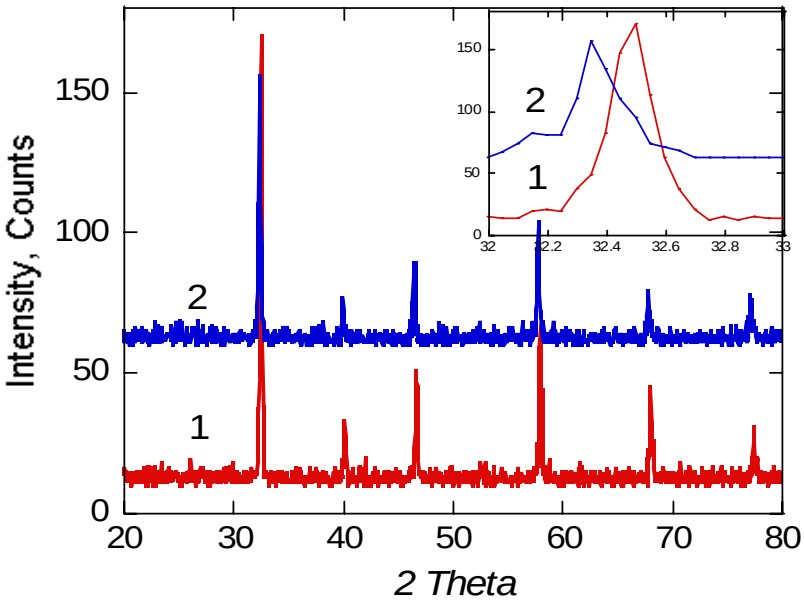

Fig 7: X-ray analysis of fractured OTM membranes under combined elevated temperature and pressure loading. 1) 25 PSI and 2)50 PSI.

The fractured samples were powdered and analyzed in a XRD for phase composition and analysis. The analysis indicated that the powder retained the perovskite (pseudo?) structure. However, there was a minor shift towards the left in the major peak angle. Slow scan analysis (not shown here) did reveal that the major peak was composed of several minor peaks indicating possible decomposition and phase transitions.

TGA/DTA analysis

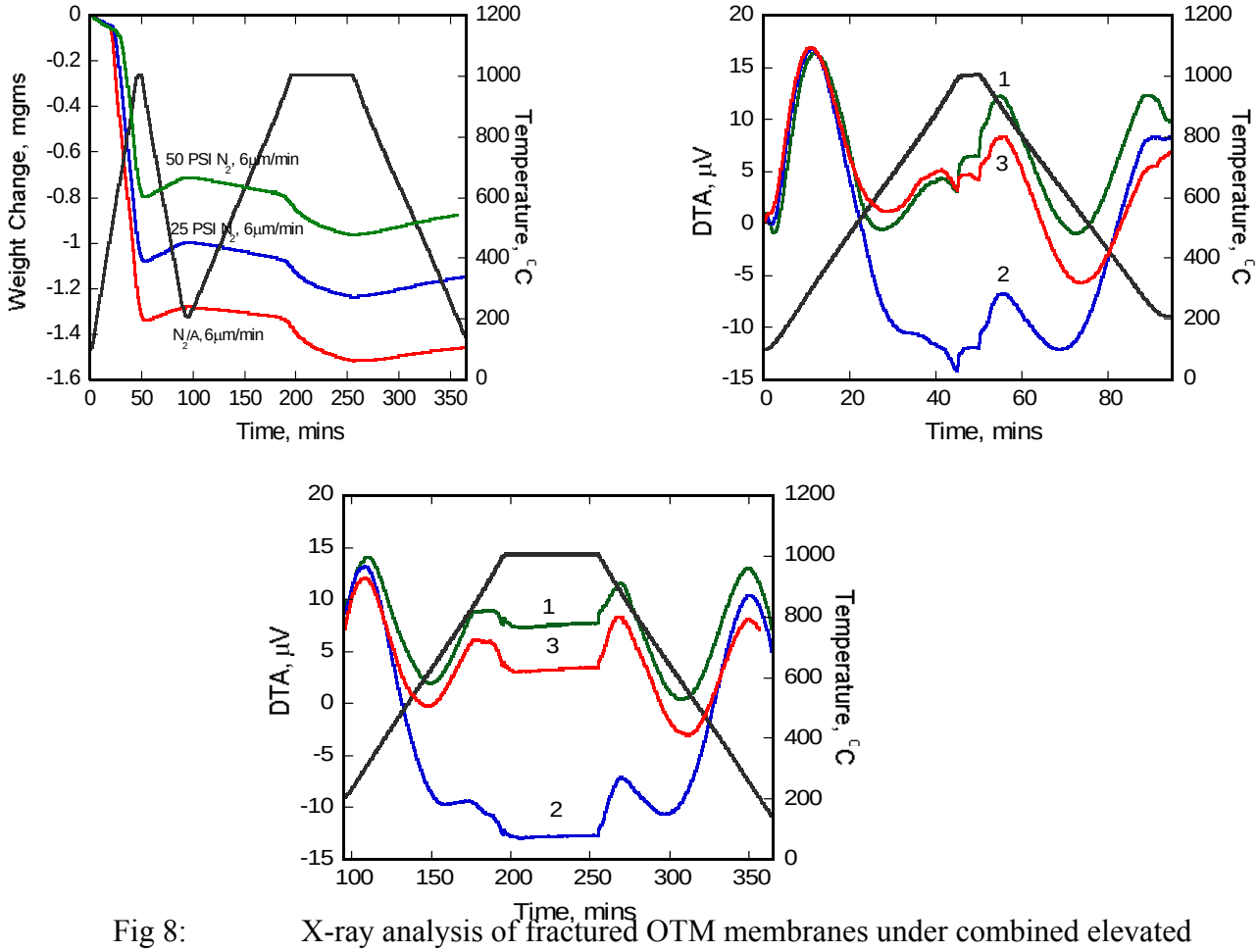

Fig 8: X-ray analysis of fractured OTM membranes under combined elevated temperature and pressure loading. 1) 25 PSI and 2)50 PSI.

As from earlier studies, the samples were analyzed in a TGA to determine the extent of stoichiometry and also to check for transitions if any. As shown in Fig 8, the second peak indicating a secondary transition (~915-950°C)was stronger in materials fractured in N_2 at 25 PSI and 50 PSI respectively.

The change in the material stoichiometry as calculated from weight change measurements, are indicated in table 1. Further drop in stoichiometry is reflected by change in 3-δ values to 2.64 and 2.63 from a equilibrium value of 2.7.

Table 1: Weight loss and DTA peaks in sample fracture in N_2 at elevated temperature and pressure.

	Wt loss	DTA (peak 1)	DTA (peak 2)	3-δ
6μm/min N2/Air 1000C	450ºC	333ºC	847ºC	2.69
Fractured in N2 at 25PSI, 1000ºC	625ºC	314ºC	916ºC	2.64
Fractured in N2 at 50PSI, 1000ºC	645ºC	295ºC	944ºC	2.63

Task 3: Measurement of Surface Activation/Reaction rates in Ion Transport Membranes using Isotope Tracer and Transient Kinetic Techniques.

Prof. Alan Jacobson, University of Houston/University of Toronto

EXPERIMENTAL

Most of the work at UH this quarter has been directed towards building an electrochemical cell for Seebeck measurements. The electrochemical cell is shown schematically in Figure 1. The top and bottom parts of the cell were composed of a pure ionic conductor, 8-wt% polycrystalline yttria-stabilized zirconia (YSZ, TZ-8Y) disc. The YSZ discs were sintered at 1450 °C for 4 h in air with a 2 °C per minute heating and cooling rate. Both sides of the YSZ disk were connected to Pt wires (0.005-inch diameter) using Pt meshes (150 × 150 mesh, 0.002-inch wire diameter, Unique Wire Weaving Co., Inc.) and Pt paste (Engelhard 6926). The top YSZ disk was used for monitoring the pO_2 and the bottom one was used for pumping the oxygen in/out of the cell. Air was used as the reference gas. The Pt wires connected to the rectangular sample bar were brought out via the glass rings. The gas- tight seals were made by heating the cell above the softening temperature (821 °C) of the glass rings. The total height of the cell was less than 45 mm after sealing.

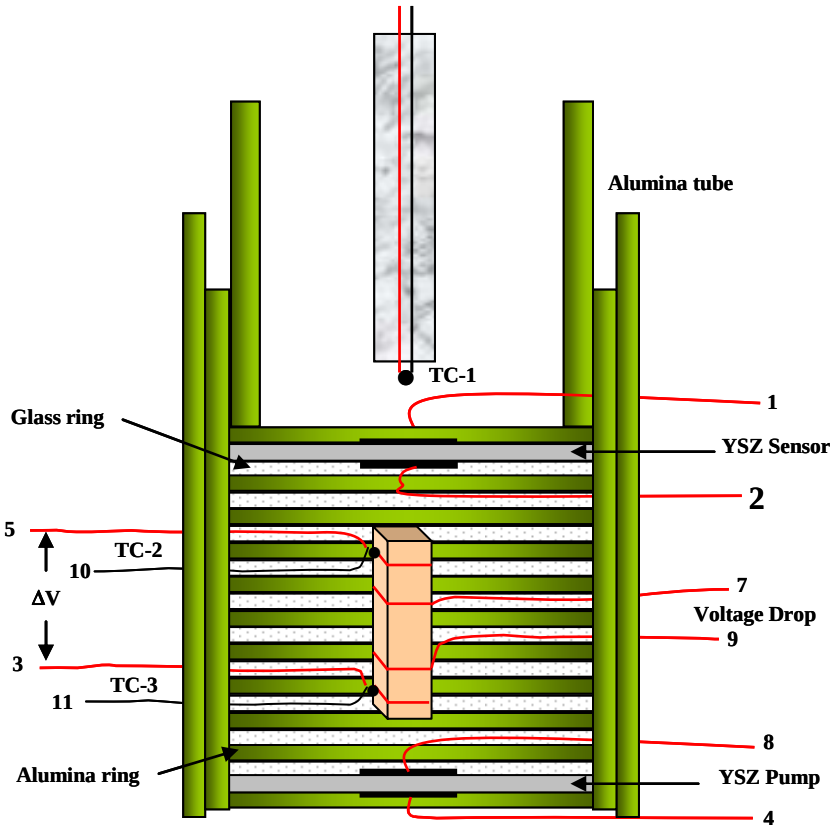

Figure 9 Electrochemical cell used for thermo-power measurements

A rectangular bar with dimensions 0.17 × 0.18 × 1.98 cm was cut from a sample that was sintered at 1400 °C. The pump current was introduced by a 2400 SourceMeter (Keithley) and the EMF of the sensor and pump were monitored by a 2000-20 multimeter (Keithley). Three R-type thermocouples were used to monitor the temperature. One thermocouple is for the vertical furnace and other two were attached to both ends of the sample in the electrochemical cell. Cold junction compensators are connected to R-type thermocouples in order to read an accurate temperature difference. We used the natural temperature gradient along the cell. Normally this is ~ 3 °C/cm but can be varied by shifting the cell along the furnace. The EMF values between two Pt wires of the thermocouples were monitored by 2182 nano-voltameter (Keithley) with the equilibrium criteria of $\leq 5 \times 10^{-5}$ μV/min and less than a half order difference between sensor and pump pO_2.

Measurements are currently being made on LSFTO in a cell as a function of temperature and pressure at $750 \leq T \leq 1000$ °C and $\sim 10^{-17} \leq pO_2 \leq 0.3$ atm, respectively. All data points have obtained manually in order to maintain a stringent equilibrium criterion. As expected it takes

more than 7 hours to obtain one data point especially in the middle of pO_2 region due to its extremely slow equilibrium kinetics.

The other experimental techniques used to generate the results reported here have been described in previous quarterly reports

RESULTS AND DISCUSSION

University of Houston

Thermopower measurements

We have continued to investigate the thermodynamic properties (stability and phase-separation behavior) and total conductivity of prototype membrane materials. The data are needed together with the kinetic information to develop a complete model for the membrane transport. We have previously reported characterization, stoichiometry, conductivity, and dilatometry measurements for samples of $La_{0.2}Sr_{0.8}Fe_{0.55}Ti_{0.45}O_{3-x}$. In this report, we describe preliminary Seebeck data and some neutron diffraction results.

Measurements are being made in the cell described above as a function of temperature and pressure at $750 \leq T \leq 1000$ °C and $\sim 10^{-17} \leq pO_2 \leq 0.3$ atm, respectively. All data points have been obtained manually in order to maintain a stringent equilibrium criterion. As expected it takes more than 7 h to obtain one data point especially in the middle of pO_2 region due to the extremely slow equilibrium kinetics. The Seebeck Coefficient (Q) was calculated from the observed Seebeck voltage by using the following equations:

$$Q = Q_{sample/Pt} - Q_{Pt} \qquad (1)$$

$$Q_{sample/Pt} = \frac{E_{sample/Pt}}{T_h - T_c} \qquad (2)$$

where Q_{Pt} is Seebeck coefficient of Pt and $E_{sample/Pt}$ is the observed Seebeck voltage. T_h and T_c are the temperatures of the hot and cold end of the sample, respectively. The values of Q_{Pt} at each temperature were taken from previous results (N. Cusak and P. Kendall, *Proc. Phys. Soc.* (*London*), **72** [5] 898-901 (1958)). The data obtained thus far at 850 °C from high to low pO_2 are shown in Figure 10. The values of Seebeck coefficient increase slightly as the pO_2 decreases and then they decrease on further decrease of pO_2. The turning point of pO_2 was $\sim 2 \times 10^{-5}$ atm with

Q ~ 40.7 μV/K at 850 °C. This behavior is frequently found in $SrFeO_{3-\delta}$ based perovskites (V. L. Kozhevnikov *et al.*, J. Solid State Chem. **158**, 320-326 (2000) and J. Mizusaki *et al.*, J. Am. Ceram. Soc. **66**, 4 247-252 (1983)).

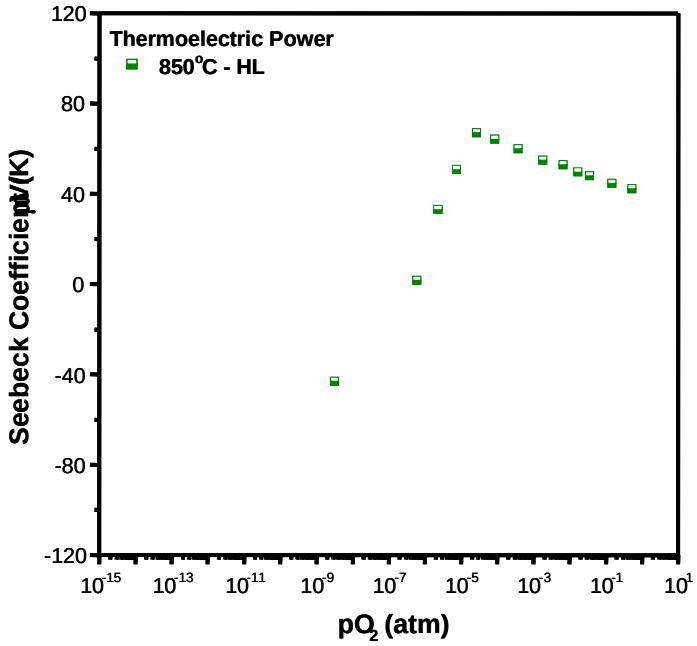

Figure 10. Preliminary thermopower results for LSFTO at 850 °C

Neutron Diffraction Measurements

In situ neutron diffraction measurements were made at Argonne National Laboratory in collaboration with Yaping Li, J. Jorgensen, and J. Richardson. Measurements were made at three temperatures and at different oxygen partial pressures. The data were taken as short scans and the fitted using the Reitveld method to obtain the lattice parameter and oxygen occupancy. One set of data taken at 1040 °C is shown in Figure 11. The Figure shows the variation in lattice parameter (left axis) as a function of time as it responds to changes in oxygen partial pressure (shown on right axis). The lattice parameter increases as the pressure is decreased. At high pO_2 values the response of the sample to changing the pO_2 is fast whereas below 10^{-4} atm the response is very slow. The response rate increase again when the pressure is dropped to 10^{-14} atm. These results mirror the previous stoichiometry and conductivity observations on this material and on other ferrites that all show very slow kinetics in the intermediate pressure range. We understand in part the origin of this effect and more details will be given in the next report. From the fits to the neutron diffraction data, the stoichiometry was determined at each of the pO_2

ranges. The results are shown in Figure 4 where the neutron diffraction values are plotted on top of the stoichiometry data measured by coulometric titration. The neutron diffraction data are in good agreement with the coulometric titration data except in the intermediate pressure region as anticipated from the previous results.

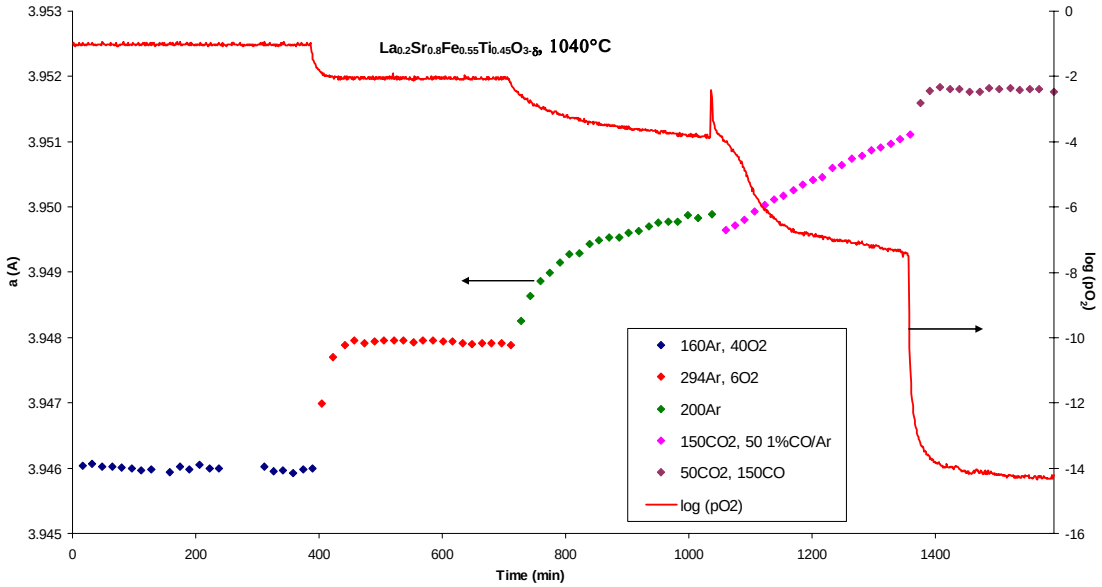

Figure 11 . In situ Neutron Diffraction Data for $La_{0.2}Sr_{0.8}Fe_{0.55}Ti_{0.45}O_{3-\delta}$ at 1040 °C

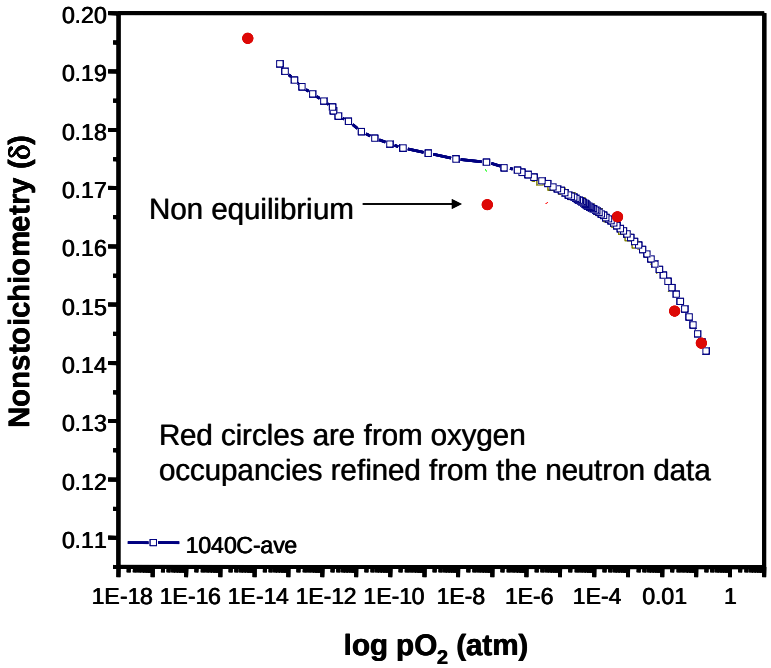

Figure 12 Comparison of the oxygen stoichiometry measure by neutron diffraction and coulometric titration.

University of Toronto

Isotope Transient Studies at Steady State - Summary of experimental progress:

Our last report described:

LSCF-6428 study: The continuing analysis of data from the LSCF-6428 study. For the quenched membrane data, we reanalyzed regions of the quenched membrane with better resolution and signal/noise. We used recently written data manipulation codes to allow us to retrieve isotope profiles from the SIMS data obtained on the tubular membrane geometry.

LSCrF-2828 studies under air separation mode: A series of isotope transients under air separation mode (small gradient) were completed on the membrane of LSCrF-2828 at 900°C. As previously described, the reversibility of oxygen activation at the air side can be obtained by observing the exchange of oxygen from the solid into the air after the administration of the isotope labeled pulse. A reverse flux will introduce ^{18}O isotope into the air, now with natural abundance, from the newly labeled solid.

LSCrF-2828 studies under syngas generation mode:

Low pO_2 atmospheres based on with CO - CO_2 mixtures were used for the first time on the LSCrF-2828 membrane to produce the gradients which exist under syngas generation conditions. Two CO:CO_2 mixtures were studied and the membrane quenched during the final isotope transient in order to obtain the developed internal isotope profile.

Air separation transients: The table below shows the conditions for isotope transients performed under low gradient (air separation mode):

p'O_2	p"O_2	O_2 flux sccm/cm_2
0.21	0.031	0.181
1.00	0.021	0.328
0.05	0.007	0.110
0.21	0.005	0.270
0.21	0.027	0.160
0.21	0.015	0.230

These transients were fit to the 1-D transport model. As Figure 13 shows, the oxygen diffusivity did not show a significant dependence on the average oxygen activity in the membrane over this modest range.

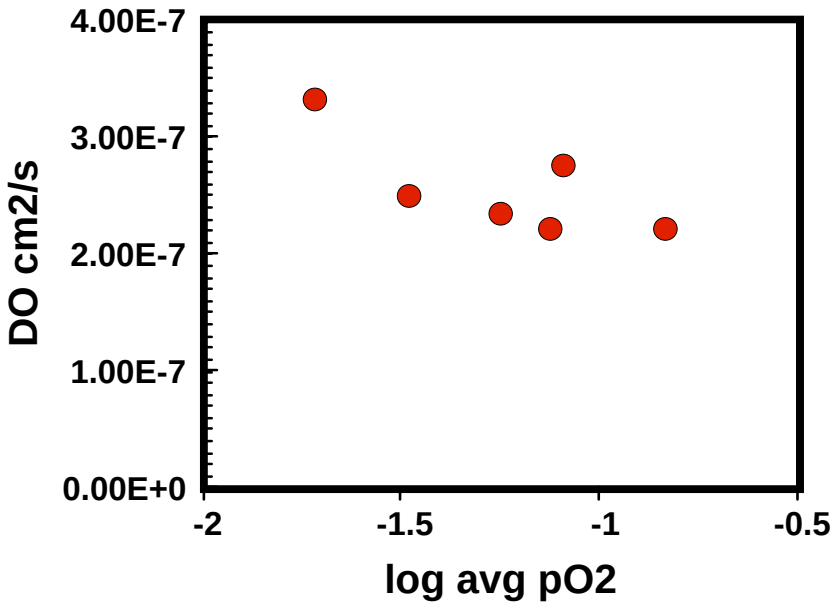

Figure 13: Oxygen diffusion coefficients, D_O , measured as a function of the average oxygen activity for the air-separation experiments.

The derived values of the forward oxygen surface activation rate coefficient for these same fits are shown in Figure 14 as a function of the air-side oxygen partial pressure. The cluster of points at 0.2 show some variability with the value of pO_2", the oxygen partial pressure on the delivery

side. The expected systematic variation, showing higher forward rate coefficients with increasing gradient across the membrane is not evident in the data.

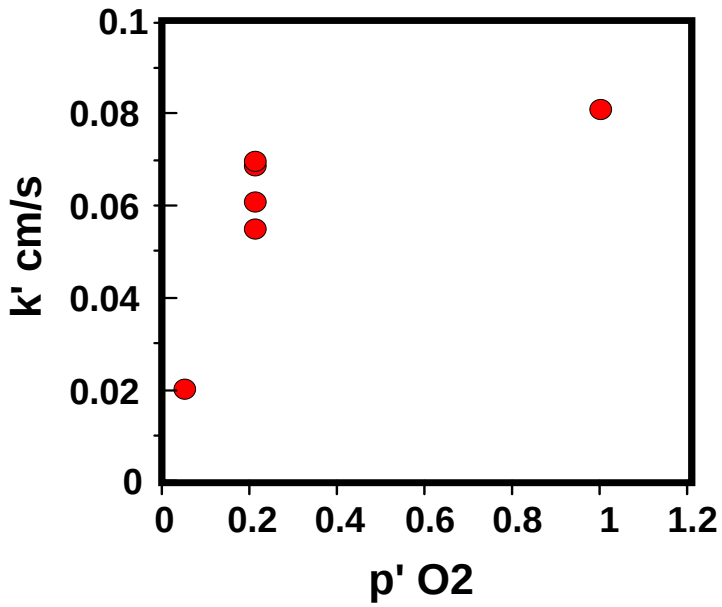

Figure 14 The forward oxygen surface activation rate coefficients
The error estimates on these fits are obtained by stochastic techniques and are still being defined.

High gradient experiments (CO_2/CO atmospheres on delivery side)

The first high gradient experiment involved a sweep gas with Ar:CO_2:CO = 90:10:1

The isotope transients of this condition are shown in Figure 15 below. Molecular oxygen appeared on the sweep side of the membrane. Oxygen recombination was sufficiently fast to compete with CO oxidation for oxygen removal on the sweep side. This is consistent with our earlier IEDP measurements showing CO :CO_2 redox exchange rates being similar to oxygen activation on these materials. The activity gradient in the membrane was therefore modest and similar to the air separation experiments. The oxygen flux to both processes was also similar (0.21 sccm at 900^{O}C). The isotope composition of the CO shows that the redox exchange is not equilibrated under these conditions.

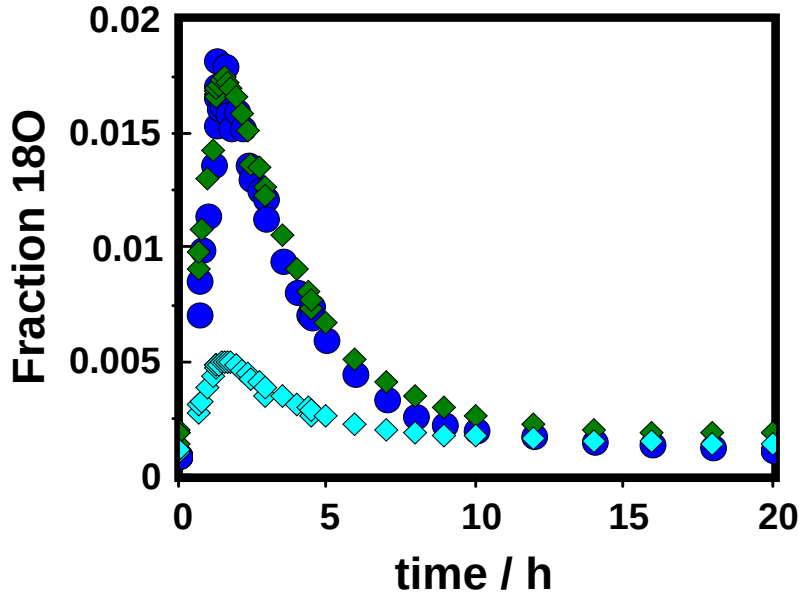

Figure 15: Isotope fraction in CO (diamonds peaking at 0.005) and in carbon dioxide (diamonds peaking at 0.02) and molecular oxygen (circles) during an isotopic transient on LSCrF 2828 membrane at $900^{O}C$.

When the gas admitted was 50% CO, the membrane switched to high gradient – high flux mode. Figure 16 shows the isotopic transient for this experiment. The time scale is much shorter, in agreement with the substantially higher oxygen flux (2.54 sccm). Under these conditions, no molecular oxygen is seen. If the entire delivery surface is at sufficient low oxygen potential, molecular oxygen formation is thermodynamically prohibited, consistent with our observations. Furthermore, the redox exchange between CO and CO2 is still largely irreversible, since the isotope content in CO is lower than in carbon dioxide, which is known to be in isotopic equilibrium with the surface.

The oxygen activation on the air side was less reversible in the presence of a higher gradient, and the forward coefficient from the model fit was somewhat higher than those

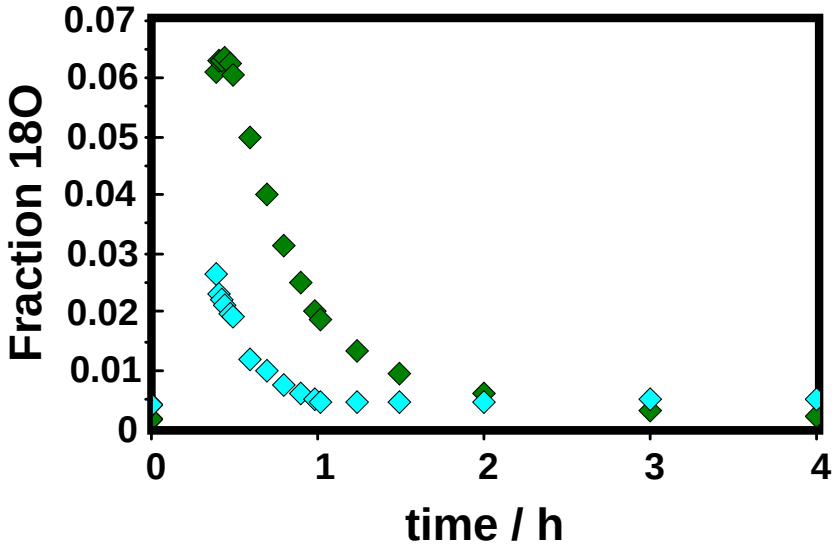

Figure 16: Isotope transient in CO (lower diamonds) and CO_2 (higher diamonds) at 900^{O}C.

from the air separation experiments. This is consistent with a higher defect density at the surface under the higher gradient, resulting in a higher oxygen activation rate coefficient. The fit value of D_O is also somewhat higher in this high gradient condition (7 versus 2.5 x 10^{-7} cm^2/s). Again the uncertainties in the fit will be more rigorously defined in work reported in the next quarter.

Quenched profile:

The oxygen – 18 SIMS map of the cross section of the membrane is shown in Figure 17. The schematic shows how the quenched membrane was cut for profile measurement. The cracks seen in the figure developed during the quench, and did not exist during the isotope transient. This is clear from the absence of isotopic anomalies near the cracks as have been seen in some IEDP experiments previously. An axial profile is also shown in the upper left part of the figure. These profiles are currently being modeled, but show an indication of a variation of D across the membrane.

Technical improvements: The use of GCMS will be introduced to allow us to measure small quantities of ^{18}O in CO without the interfering signal of fragmented CO_2 which arises in the online MS analysis.

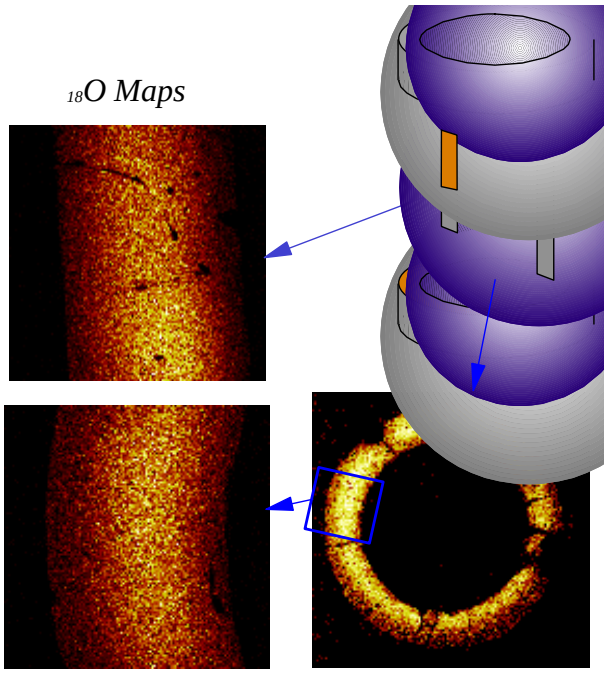

Figure 17: Quenched isotope (O-18) distribution in the LSCrF 2828 membrane. The quench was performed at 900OC under high oxygen gradient conditions as described above (see Figure 16).

Dissemination: Two abstracts based on the work here have been submitted to the December MRS Meeting in Boston and will be submitted to the International Solid State Ionics conference to be held in Baden-Baden Germany July 2005.

CONCLUSIONS

For a detailed analysis of the transport properties Ti doped LSF further studies are need to be by *In situ* neutron diffraction. Presently, the space group of R3c yields a better refinement than a cubic structure of Pm3m. The oxygen occupancy is observed to be nearly 3 in the region from room temperature to 700ºC, above which the occupancy decreased due to oxygen loss. These have implication on the thermal expansion of the crystal and needs to be correlated with physical measurements on Ti doped LSF.

Stable crack growth and fracture in LSFCO-OTM material can be achieved by using a bridge-compression technique for generating pre-cracks from indented flaws. The crack growth behavior at room temperature is well reproduced at elevated temperature. Modified TG-DTA studies present further evidence on the presence of previous thermal or stress history in approximating changes in stoichiometry. Some of the transitions appear to be reversible in nature.

Further analysis of data is of vital concern for justifying many of the conclusion that could be drawn from work in the present quarter. A tentative hire of a new postdoc to help with the program has been made, but delayed until later this year. Particular attention will be paid to any resolution of the variation in DO across the membrane in the quenched experiment.

REFERENCES

N/A

BIBLIOGRAPHY:

N/A

LISTS OF ACRONYMS AND ABBREVIATIONS:

OTM	Oxygen Transport Membrane
LSFCO	Lanthanum Strontium Iron Chromium Oxide ($La_{0.2}Sr_{0.8}Fe_{0.8}Cr_{0.2}O_{3-\delta}$)
LSF	Lanthanum Strontium Ferrite ($La_xSr_{1-x}FeO_{3-\delta}$)
LSCF	Lanthanum Strontium Cobalt Iron Oxide ($La_xSr_{1-x}Fe_{1-y}Co_yO_{3-\delta}$)
L2SF55T	Lanthanum Strontium Iron Titanium Oxide ($La_{0.2}Sr_{0.8}Fe_{0.55}Ti_{0.45}O_{3-\delta}$)
YSZ	Yttria stabilized zirconia
XRD	X-ray diffraction
LSFTO	$La_{0.2}Sr_{0.8}Fe_{0.55}Ti_{0.45}O_{3-\delta}$
LSCF-6428	$La_{0.6}Sr_{0.4}Co_{0.2}Fe_{0.8}O_{3-\delta}$
LSCrF-2828	$La_{0.2}Sr_{0.8}Cr_{0.2}Fe_{0.8}O_{3-\delta}$
IEDP	Isotope exchange and depth profiling
SIMS	Secondary Ion Mass Spectroscopy